Uncovering the mechanism of the hydrogen poisoning on Ru nanoparticles via density functional theory calculations

David S. Rivera Rocabado [1,*], Mika Aizawa [1], Tomohiro G. Noguchi [2], Miho Yamauchi [2,3,4], and Takayoshi Ishimoto [1,*]

[1] *Graduate School of Advanced Science and Engineering, Hiroshima University, 1-4-1 Kagamiyama, Higashi-Hiroshima 739-8527, Japan*

[2] *International Institute for Carbon-Neutral Energy Research (WPI-I2CNER), Kyushu University, Motooka 744, Nishi-ku, Fukuoka 819-0395, Japan*

[3] *Institute for Materials Chemistry and Engineering (IMCE), Motooka 744, Nishi-ku, Fukuoka 819-0395, Japan*

[4] *Advanced Institute for Materials Research (WPI-AIMR), Tohoku University, 2-1-1 Katahira, Aoba-ku, Sendai 980-8577, Japan*

-0.468   -0.555   -0.594   -0.637   -0.716

-0.825   -1.291   -1.592   -1.794   -1.854
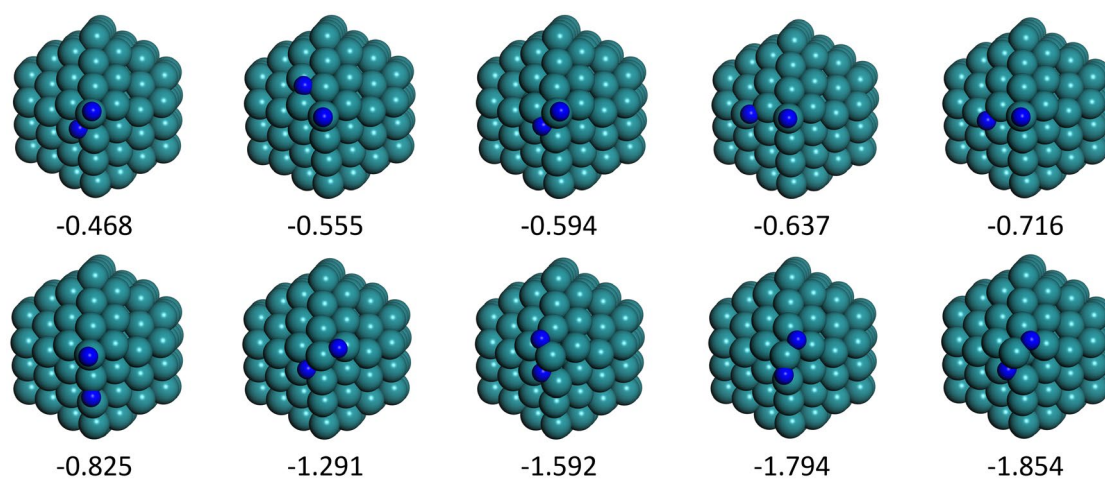
Figure S1. Dissociated configurations from the most stable vertical N_2 adsorption on the top site. The dissociative energy values are shown, the units are eV.
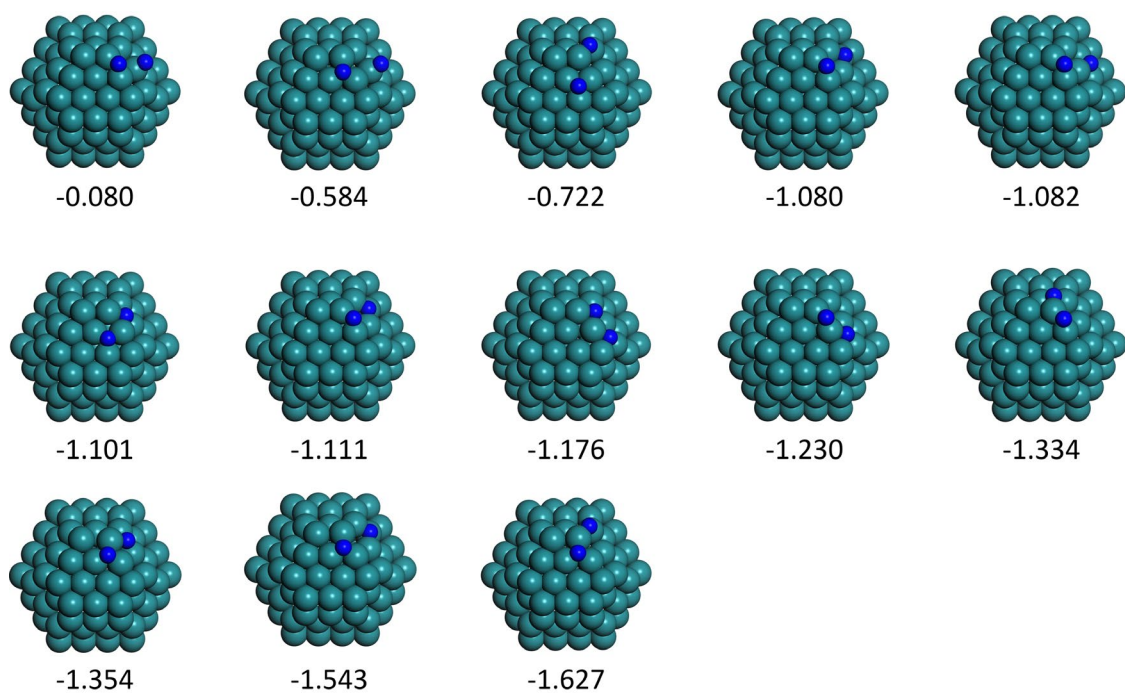
-0.080   -0.584   -0.722   -1.080   -1.082

-1.101   -1.111   -1.176   -1.230   -1.334

-1.354   -1.543   -1.627

Figure S2. Dissociated configurations from the most stable horizontal N_2 adsorption on a 4F site. The dissociative energy values are shown, the units are eV.
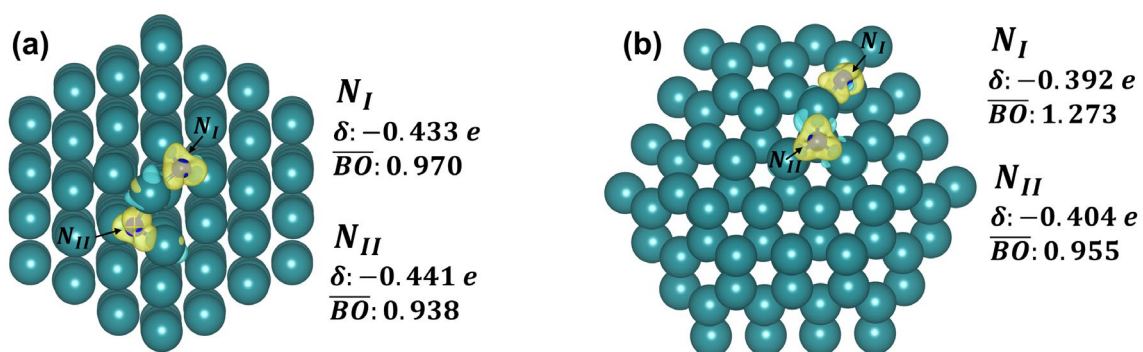
(a) N_I — $\delta: -0.433\ e$, $\overline{BO}: 0.970$; N_{II} — $\delta: -0.441\ e$, $\overline{BO}: 0.938$

(b) N_I — $\delta: -0.392\ e$, $\overline{BO}: 1.273$; N_{II} — $\delta: -0.404\ e$, $\overline{BO}: 0.955$

Figure S3. Electron density difference for the dissociated N_2 from the most stable (a) N_2 vertically adsorbed on top and (b) N_2 horizontally adsorbed on 4F. The charge (δ) of the N atoms and averaged Ru-N bond orders ($\overline{BO}$) are also shown. Yellow and blue regions indicate positive and negative electron density, respectively. The isosurface level is 0.005.

-0.516	-0.591	-0.703	-0.726	-0.752
-0.765	-0.800	-0.915	-0.934	-0.952
-0.968	-1.278	-1.333	-1.348	
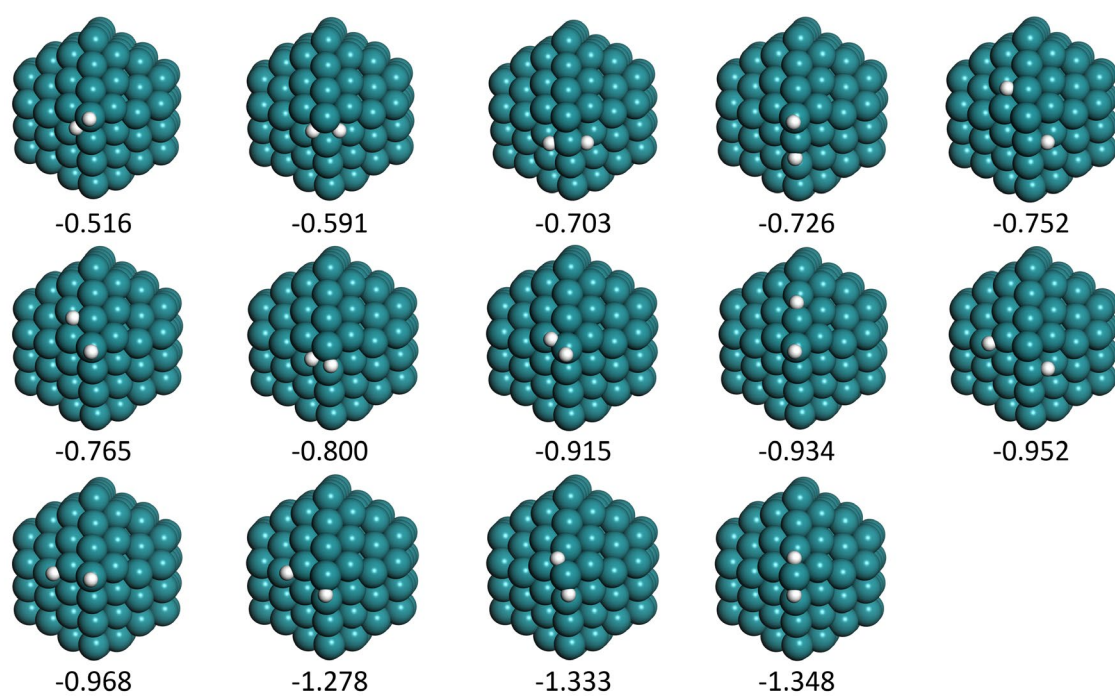
Figure S4. Dissociated configurations from the most stable horizontal H_2 adsorption on top of a vertex site. The dissociative energy values are shown, the units are eV.
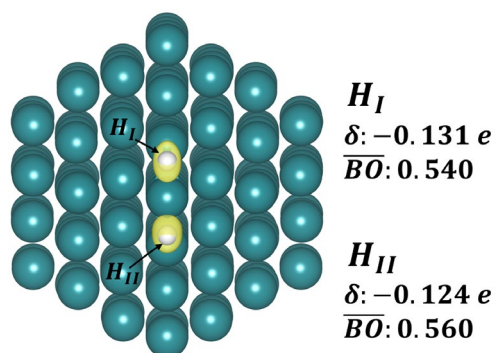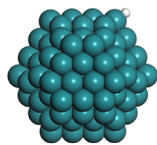
$$H_I$$
$$\delta: -0.131\ e$$
$$\overline{BO}: 0.540$$

$$H_{II}$$
$$\delta: -0.124\ e$$
$$\overline{BO}: 0.560$$

Figure S5. Electron density difference for the dissociated H_2. The charge (δ) of the H atoms and averaged Ru-H bond orders ($\overline{BO}$) are also shown. Yellow and blue regions indicate positive and negative electron density, respectively. The isosurface level is 0.005.

E_{bind} (eV)	-2.512
ν (cm^{-1})	1869
$\bar{d}_{Ru-H}$ (Å)	1.646
ΣBO_{Ru-H}	1.021
$\delta_H(e)$	-0.142

Figure S6. H atom binding on the top site of Ru$_{153}$. Binding energy (E_{bind}), vibrational frequency (ν), average interatomic Ru-H distance ($\bar{d}_{Ru-H}$), the sum of Ru-H bond order (Σ_{Ru-H}), and the charge of the H (δ_H) are shown.
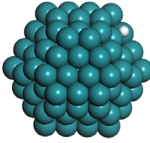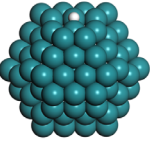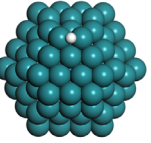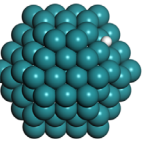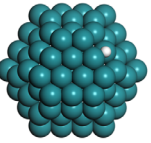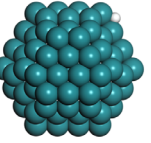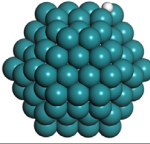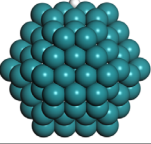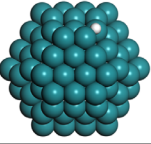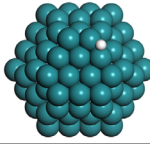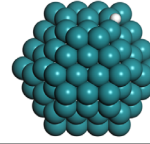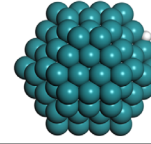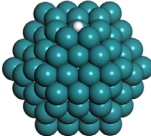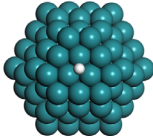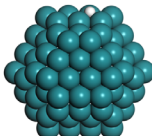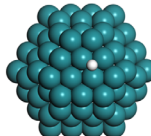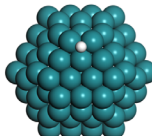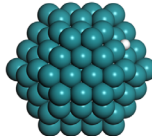
E_{bind} (eV)	-2.499	-2.734	-2.760	-2.773	-2.782	-2.849
ν (cm^{-1})	1374	1355	1275	1396	1331	1318
$\bar{d}_{Ru-H}$ (Å)	1.807	1.791	1.815	1.811	1.810	1.816
ΣBO_{Ru-H}	1.145	1.159	1.154	1.124	1.169	1.131
$\delta_H(e)$	-0.092	-0.084	-0.114	-0.074	-0.109	-0.123

E_{bind} (eV)	-2.871	-2.918	-2.933	-2.969	-2.969	-2.973
ν (cm^{-1})	1363	1360	1344	1363	1353	1313
$\bar{d}_{Ru-H}$ (Å)	1.814	1.793	1.816	1.821	1.801	1.791
ΣBO_{Ru-H}	1.136	1.151	1.137	1.139	1.137	1.161
$\delta_H(e)$	-0.107	-0.088	-0.118	-0.126	-0.096	-0.111

Figure S7. H atom binding on the bridge sites of Ru₁₅₃. Binding energies (E_{bind}), vibrational frequencies (ν), average interatomic Ru-H distance ($\bar{d}_{Ru-H}$), the sum of Ru-H bond order (Σ_{Ru-H}), and the charge of the H (δ_H) are shown.

8

E_{bind} (eV)	-2.751	-2.764	-2.779	-2.789	-2.793	-2.861
ν (cm^{-1})	1213	1118	1216	1168	1164	1240
$\bar{d}_{Ru-H}$ (Å)	1.917	1.892	1.914	1.906	1.920	1.901
ΣBO_{Ru-H}	1.176	1.172	1.157	1.165	1.186	1.163
$\delta_H(e)$	-0.094	-0.049	-0.068	-0.066	-0.102	-0.064
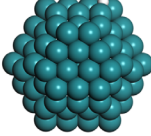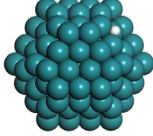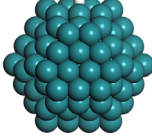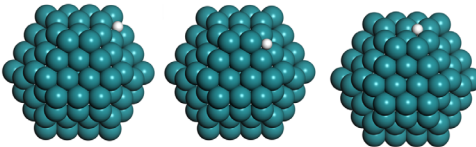
E_{bind} (eV)	-2.867	-2.878	-2.913
ν (cm^{-1})	1301	1187	1247
$\bar{d}_{Ru-H}$ (Å)	1.960	1.899	1.920
ΣBO_{Ru-H}	1.162	1.171	1.171
$\delta_H(e)$	-0.101	-0.068	-0.077

Figure S8. H atom binding on the 3F sites of Ru$_{153}$. Binding energies (E_{bind}), vibrational frequencies (ν), average interatomic Ru-H distance ($\bar{d}_{Ru-H}$), the sum of Ru-H bond order (Σ_{Ru-H}), and the charge of the H (δ_H) are shown.

E_{bind} (eV)	-2.554	-2.763	-2.770
ν (cm^{-1})	959	930	967
$\bar{d}_{Ru-H}$ (Å)	2.040	2.082	2.055
ΣBO_{Ru-H}	1.219	1.189	1.177
$\delta_H(e)$	-0.072	-0.091	-0.065

Figure S9. H binding on 4F sites of Ru$_{153}$. Binding energies (E_{bind}), vibrational frequencies (ν), average interatomic Ru-H distance ($\bar{d}_{Ru-H}$), the sum of Ru-H bond order (Σ_{Ru-H}), and the charge of the H (δ_H) are shown.
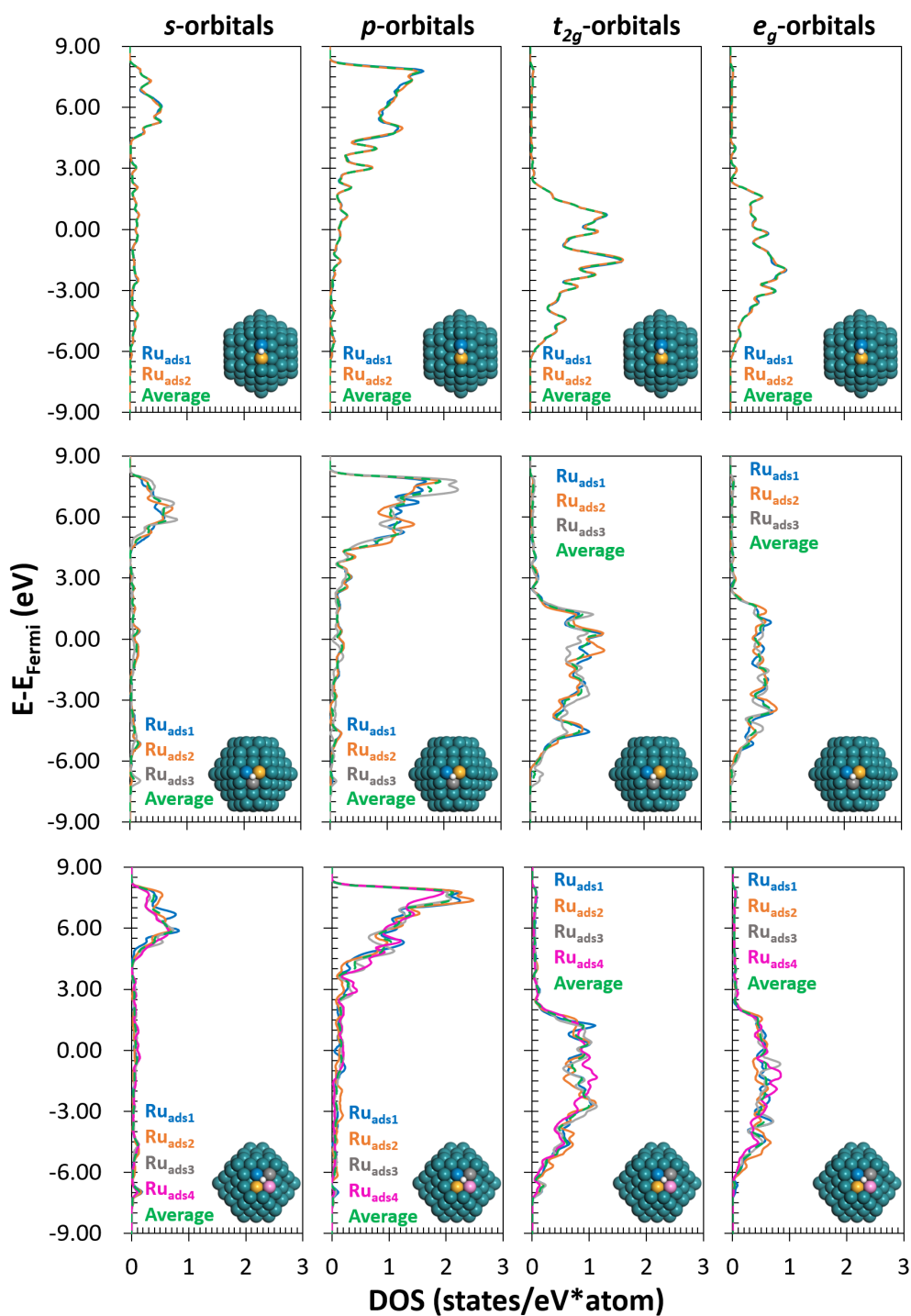
Figure S10. Comparison between the DOS profiles of the individual Ru atoms and their average DOS for the most stable structures of the H atom binding on the bridge, 3F, and 4F sites. Different colored solid lines and the broken green line represent each Ru atom's DOS at the adsorption site and the averaged DOS of the Ru atoms at the adsorption site, respectively.
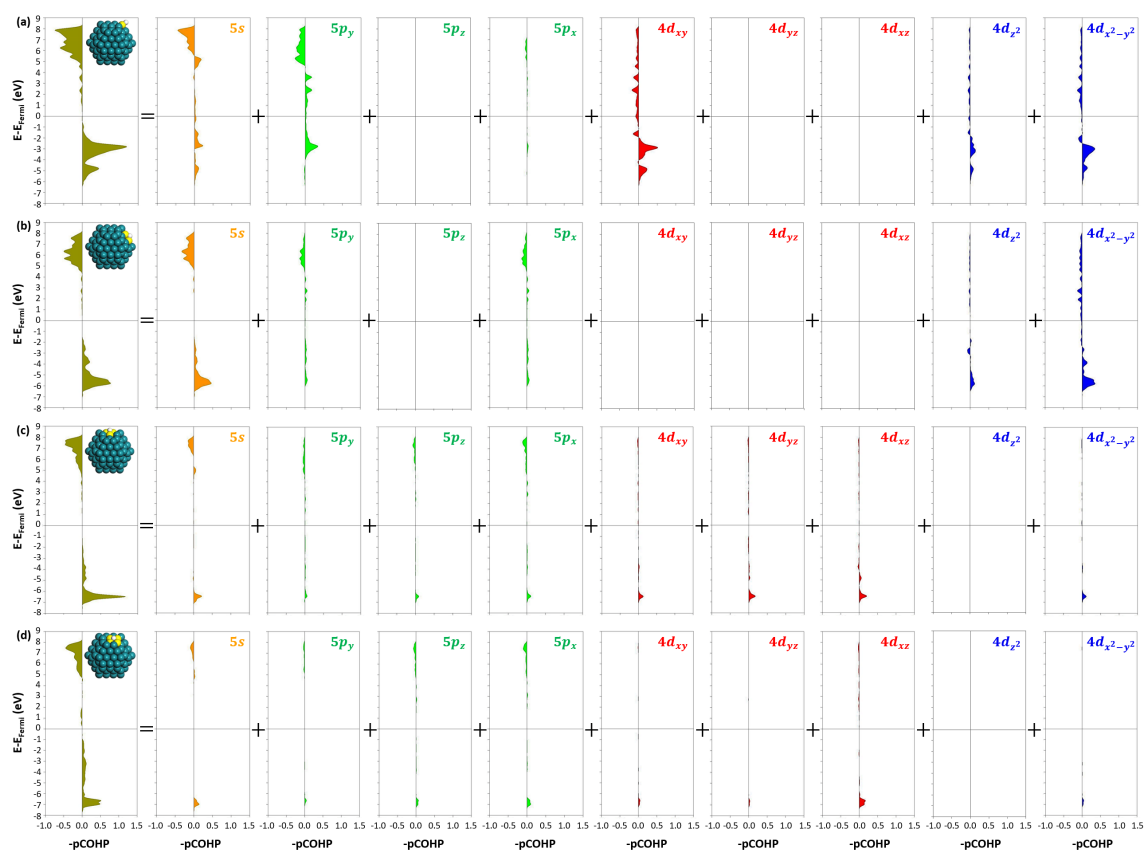
Figure S11. Atomic orbital decomposition of the H atom binding on the most stable (a) top, (b) bridge, (c) 3F, and (d) 4F sites of Ru_{153} by the projected crystal orbital Hamiltonian population. The H atom is presented with white spheres, and the interacting Ru atoms are shown with yellow spheres.
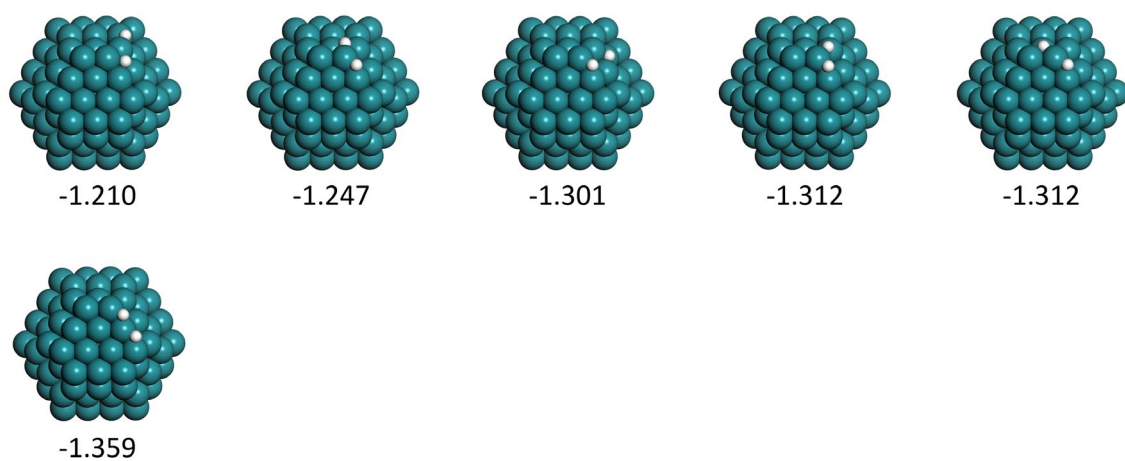
-1.210   -1.247   -1.301   -1.312   -1.312

-1.359

Figure S12. Dissociated H atoms on the same sites required for the N$_2$ adsorption and dissociation from the 4F site. The dissociative energy values are shown, the units are eV.

Strain in the surface atoms of Ru₁₅₃

In Figure S13 are shown the Ru₁₅₃ and hexagonal close-packed (HCP) structure of bulk Ru with their respective averaged interatomic Ru-Ru distances. The optimization of the HCP bulk Ru was performed via a spin-polarized calculation with a plane-wave cutoff energy of 600 eV. The convergence criteria were 10^{-5} eV/atom and 10^{-6} eV/atom for ionic steps and the self-consists-field iterations, respectively, with 16 × 16 × 10 Monkhorst–Pack k-point mesh for the Brillouin zone integration where all the atoms and the crystal volume were allowed to relax. After the optimization, the calculated lattice parameters, a = 2.715 and c = 4.279 Å, were in good agreement with the experimental values a = 2.706 and c = 4.282 Å. The strain of the Ru₁₅₃ surface atoms relative to the interatomic Ru-Ru distance in HCP bulk Ru was calculated as:

$$strain = \frac{d_{surface} - d_{bulk}}{d_{bulk}} * 100 \tag{S1}$$

where $d_{surface}$ and d_{bulk} are the average interatomic distances at the surface of Ru₁₅₃ and HCP bulk Ru. The negative value of the strain, -1.49%, corroborates the usual compressive strain that nanoparticles exhibit compared to the bulk structure.
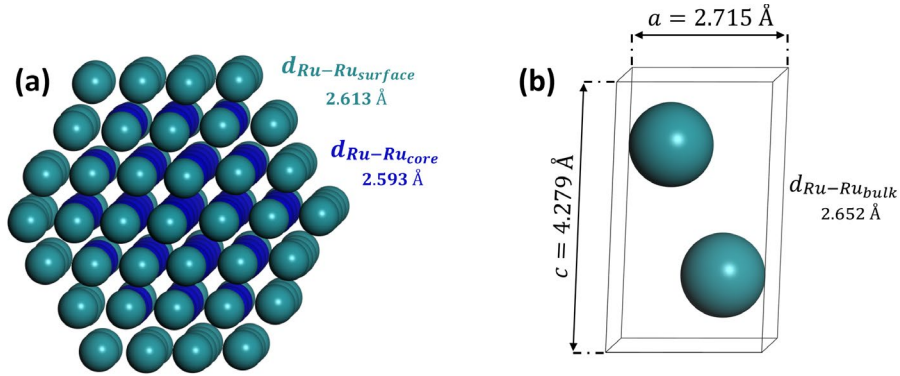

Figure S13. Interatomic Ru-Ru distances of (a) Surface atoms of Ru₁₅₃ and (b) HCP bulk Ru.